

## Mean field phase diagram of an $SU(2)_L \times SU(2)_R$ lattice Higgs-Yukawa model at finite $\lambda$

Craig Pryor

*Sierra Center for Physics, 939 N. Van Ness Ave. Suite 2, Fresno, California 93728*

(Received 27 April 1995; revised manuscript received 28 July 1995)

The phase diagram of an  $SU(2)_L \times SU(2)_R$  lattice Higgs-Yukawa model with finite  $\lambda$  is constructed using mean field theory. The phase diagram bears a superficial resemblance to that for  $\lambda = \infty$ ; however, as  $\lambda$  is decreased the paramagnetic region shrinks in size. For small  $\lambda$  the phase transitions remain second order, and no new first order transitions are seen.

PACS number(s): 11.15.Ha, 11.15.Ex

Recent experimental evidence of a top quark with mass  $\approx 175$  GeV [1] indicates that its Yukawa coupling is of order 1, possibly making nonperturbative effects significant. Lattice Higgs-Yukawa theories provide a way of studying nonperturbative physics of theories containing interacting scalars and fermions, although the technical problems associated with chiral fermions restricts us to vector theories.

Most of the work on Higgs-Yukawa theories has dealt with the limit in which the Higgs field is radially frozen ( $\lambda = \infty$ ). Such models have been studied both analytically [2-4] and using Monte Carlo simulations [5] for various gauge groups. Radially active (finite  $\lambda$ ) Higgs models without fermions have also been thoroughly examined [6,7]; however, relatively little work has been done on the problem including fermions [8]. In this paper I estimate the phase diagram of the  $SU(2)_L \times SU(2)_R$  Higgs-Yukawa theory for the full range of  $\lambda$  and the Yukawa coupling. The calculations are performed using the mean field approximation (MFA) [9], with the fermions included in the manner used by Stephanov and Tsypin for the radially frozen theory [3].

The action for the model in  $d$  dimensions is  $S = S_F + S_H + V_H$ ,

$$\begin{aligned}
 S_F &= \frac{1}{2} \sum_{x,\mu} (\bar{\psi}_x \gamma_\mu \psi_{x+\mu} - \bar{\psi}_{x+\mu} \gamma_\mu \psi_x) \\
 &\quad + y \sum_x \bar{\psi}_x (P_R \rho_x \Phi_x + P_L \rho_x \Phi_x^\dagger) \psi_x \\
 &= \sum_{xy} \bar{\psi}_x [K_{xy} + y(P_R \rho_x \Phi_x + P_L \rho_x \Phi_x^\dagger) \delta_{xy}] \psi_y \\
 &= \sum_{xy} \bar{\psi}_x M_{xy} \psi_y, \tag{1}
 \end{aligned}$$

$$S_H = -\kappa \sum_{x,\mu} \frac{1}{2} \text{tr} (\rho_x \Phi_x^\dagger \rho_{x+\mu} \Phi_{x+\mu} + \rho_{x+\mu} \Phi_{x+\mu}^\dagger \rho_x \Phi_x), \tag{2}$$

$$V_H = \sum_x V(\rho_x) = \sum_x \lambda (\rho_x^2 - 1)^2 + \rho_x. \tag{3}$$

The fermion field  $\psi_x$  is an  $SU(2)$  doublet,  $P_{R,L} = \frac{1}{2}(1 \pm \gamma_{d+1})$ , and  $\kappa$  is the scalar hopping parameter. The scalar field has been separated into its magnitude and angular degree of freedom,  $\rho_x$  and  $\Phi_x$ , respectively, where  $\Phi_x$  is a  $2 \times 2$   $SU(2)$  matrix. We will also use the  $O(4)$  field  $\phi_x^k$  satisfying  $\phi_x^k \phi_x^k = 1$ . The two notations are related by  $\Phi_x = \phi_x^k T^k$  where  $T^k = (1, i\vec{\sigma})$ . Integrating out the fermions gives the effective action for the scalar field:

$$S_{\text{eff}} = S_H + V_H - N_F \ln \det M, \tag{4}$$

where  $N_F$  has been introduced as the number of fermion species, each having the same action  $S_F$ . The partition function for the effective scalar theory is

$$Z = \int \prod_x \rho_x^3 d\rho_x \int \prod_x D\phi_x \exp(-S_{\text{eff}}), \tag{5}$$

where  $D\phi_x$  is the  $O(4)$ -invariant group measure for  $\phi_x^k$ .

The variational form of the MFA is employed by introducing a parameter  $H^k$ , and then adding and subtracting the trial action  $\rho_x \phi_x^k H^k$  to obtain

$$\exp(-F) = \int \prod_x \rho_x^3 d\rho_x \int \prod_x D\phi_x \exp \left( -S_{\text{eff}} + \sum_x \rho_x \phi_x^k H^k - \sum_x \rho_x \phi_x^k H^k \right). \tag{6}$$

This gives the variational limit on the free energy  $F$ :

$$F \leq F_{\text{var}} = \langle S_H - N_F \ln \det M \rangle_H + \left\langle \sum_x H^k \phi_x^k \rho_x \right\rangle_H - \ln Z_H, \tag{7}$$

$$\langle A \rangle_H = Z_H^{-1} \int \prod_x d\rho_x \rho_x^3 \exp[-V(\rho_x)] \int \prod_x D\phi_x \exp\left(\sum_x H^k \phi_x^k \rho_x\right) A, \tag{8}$$

$$Z_H = \int \prod_x d\rho_x \rho_x^3 \exp[-V(\rho_x)] \int \prod_x D\phi_x \exp\left(\sum_x H^k \phi_x^k \rho_x\right). \tag{9}$$

$F_{\text{var}}$  is then minimized with respect to  $H^k$ . The integration over  $\rho_x$  is necessary since for finite  $\lambda$  the magnitude of the scalar is no longer constrained to be 1. At small  $\lambda$  the shallow scalar potential causes fluctuations about  $\rho_x = 1$  which alter the results considerably.

For small Yukawa couplings the fermionic determinant is calculated by expanding in  $y$ :

$$\begin{aligned} \langle \ln \det M \rangle_H &= \ln \det K_{xy} - \sum_{n=2,4,\dots} \frac{1}{n} y^n \sum_{x_1 \dots x_n} K_{x_1 x_2}^{-1} \dots K_{x_{n-1} x_n}^{-1} \langle \text{tr} \Phi_{x_1} \Phi_{x_2}^\dagger \dots \Phi_{x_{n-1}} \Phi_{x_n}^\dagger \rangle_H \\ &\approx \ln \det K_{xy} - \sum_{n=2,4,\dots} \frac{1}{n} \left(\frac{-2y}{d}\right)^n \sum_{x_1 \dots x_n} K_{x_1 x_2} \dots K_{x_{n-1} x_n} \langle \text{tr} \Phi_{x_1} \Phi_{x_2}^\dagger \dots \Phi_{x_{n-1}} \Phi_{x_n}^\dagger \rangle_H. \end{aligned} \tag{10}$$

The second line uses the approximation [3]

$$K_{xy}^{-1} = \frac{-2}{d} K_{xy} + O(1/d^2), \tag{11}$$

which is justified since the MFA is itself only accurate to order  $1/d$ . The determinant is then represented by a sum of closed hopping diagrams connecting sites associated with alternating  $\Phi$ 's and  $\Phi^\dagger$ 's. Previous work has approximated the fermionic determinant by including an infinite subset of hopping diagrams [3] or by expanding Eq. (10) to some finite order in  $y$  [4]. We will adopt the latter approach.

The  $\lambda = \infty$  case provides a hint in choosing how far to carry out the expansion of the fermionic determinant. Since the radially frozen theory in the MFA agrees quite well with Monte Carlo results when the free energy is expanded to order  $y^4$ , we will evaluate Eq. (10) to order  $y^4$ . It is a tedious though straightforward exercise to enumerate all such hopping diagrams in  $d$  dimensions to obtain

$$\begin{aligned} \langle \ln \det M \rangle_H &\approx \ln \det K + \frac{2d/2}{d} y^2 \text{tr} \langle \rho_x \Phi_x \rangle_H \langle \rho_x \Phi_x \rangle_H - \frac{2d/2}{2d^3} y^4 \left[ \text{tr} \langle \rho_x \Phi_x \rho_y \Phi_y^\dagger \rho_x \Phi_x \rho_y \Phi_y^\dagger \rangle_H \right. \\ &\quad \left. + 2(2d-1) \text{tr} \langle \rho_x \Phi_x \rho_x \Phi_x \rangle_H \langle \rho_x \Phi_x \rangle_H \langle \rho_x \Phi_x \rangle_H + 2(d-1) \text{tr} \langle \rho_x \Phi_x \rangle_H^4 \right], \end{aligned} \tag{12}$$

where the traces are over  $SU(2)$  indices, and the indices  $x$  and  $y$  simply indicate which  $\Phi$ 's are distinct group elements.

The various quantities of the form  $\langle A \rangle_H$  in Eq. (12) include group integrals and integrals over  $\rho$ . The group integrals are calculated to second order in  $H$  because that is all that is required to find second order critical lines. We first compute the  $O(4)$  group integrals by taking derivatives with respect to  $H$  of

$$\begin{aligned} \int D\phi_x \exp(H^n \phi_x^n \rho_x) &= 2\pi^2 [I_0(H\rho_x) - I_2(H\rho_x)] \\ &= 2\pi^2 \left( 1 + \frac{1}{8} \rho_x^2 H^2 + \frac{1}{192} \rho_x^4 H^4 \right) + O(H^6), \end{aligned} \tag{13}$$

where  $H = \sqrt{H^k H^k}$  and  $I_n(x)$  is the  $n$ th order modified Bessel function. We find

$$\int D\phi_x \exp(\rho_x H^n \phi_x^n) \phi_x^i = \frac{\pi^2}{2} \rho_x H^i + O(H^3), \tag{14}$$

$$\int D\phi_x \exp(\rho_x H^n \phi_x^n) \phi_x^i \phi_x^j = \frac{1}{12} \pi^2 \rho_x^2 H^i H^j + \delta^{ij} \left( \frac{1}{2} + \frac{1}{24} \rho_x^2 H^2 \right) \pi^2 + O(H^4). \tag{15}$$

The corresponding  $SU(2)$  group integrals are

$$\text{tr} \langle \Phi_x \Phi_x \rangle_H = -2\pi^2 + O(H^4), \tag{16}$$

$$\langle \Phi_x \rangle_H = \mathbb{1} \frac{\pi^2}{2} H \rho_x + O(H^3). \tag{17}$$

In Eq. (17) the gauge has been fixed to  $H^i = H \delta^{i0}$ .

In addition, the slightly more complicated group integral involving four  $\Phi$ 's is needed. This is calculated as

$$\begin{aligned}
 \text{tr} \int D\phi_x D\phi_y \exp(\rho_x H^n \phi_x^n + \rho_y H^n \phi_y^n) \Phi_x \Phi_y^\dagger \Phi_x \Phi_y^\dagger \\
 = (\delta^{ij} \delta^{kl} + \delta^{il} \delta^{jk} - \delta^{ik} \delta^{jl}) \int D\phi_x \exp(\rho_x H^n \phi_x^n) \phi_x^i \phi_x^k \int D\phi_y \exp(\rho_y H^n \phi_y^n) \phi_y^j \phi_y^l \\
 = -\pi^4 \left( 4 + \frac{1}{2} H^2 \rho_x^2 + \frac{1}{2} H^2 \rho_y^2 \right) + O(H^4). \tag{18}
 \end{aligned}$$

The second line relies on the fact that the trace must be separately symmetric in both  $i, k$  and in  $j, l$ . The sum over  $O(4)$  indices is computed using Eq. (15) and by again choosing the  $H^i = H\delta^{i0}$  gauge.

For computing the integrals over  $\rho$  it is useful to define

$$\begin{aligned}
 P_n &= \int_0^\infty d\rho \rho^n \exp[-V(\rho)] \\
 &= \frac{1}{2} (2\lambda)^{-\frac{n+1}{4}} \Gamma\left(\frac{n+1}{2}\right) D_{-\frac{n+1}{2}}\left(\frac{(1-2\lambda)}{\sqrt{2\lambda}}\right) \exp\left(\frac{1}{8\lambda} - \frac{1}{2} - \frac{\lambda}{2}\right), \tag{19}
 \end{aligned}$$

where  $D_{-\frac{n+1}{2}}$  is the parabolic cylinder function. The single-site partition function is then given by

$$\begin{aligned}
 Z_1 &= 2\pi^2 \int_0^\infty d\rho_x \rho_x^3 \exp[-V(\rho_x)] [I_0(\rho_x H) - I_2(\rho_x H)] \\
 &= 2\pi^2 \int_0^\infty d\rho_x \rho_x^3 \exp[-V(\rho_x)] \left[ 1 + \frac{1}{8} H^2 \rho_x^2 \right] + O(H^4) \\
 &= 2\pi^2 \left( P_3 + \frac{1}{8} H^2 P_5 \right) + O(H^4). \tag{20}
 \end{aligned}$$

Similarly, the integrals making up Eq. (7) are given by

$$\langle \rho_x \Phi \rangle_H = \frac{1}{2} \left[ \frac{P_5}{2P_3} H + O(H^3) \right], \tag{21}$$

$$\text{tr} \langle \rho_x \Phi \rho_x \Phi \rangle_H = \frac{-P_5}{P_3} + \frac{P_5^2}{8P_3^2} H^2 + O(H^4), \tag{22}$$

$$\text{tr} \langle \rho_x \Phi_x \rho_y \Phi_y^\dagger \rho_x \Phi_x \rho_y \Phi_y^\dagger \rangle_H = \left( \frac{P_5}{P_3} \right)^2 + H^2 \frac{P_3 P_5 P_7 - 3P_5^3}{12P_3^3} + O(H^4). \tag{23}$$

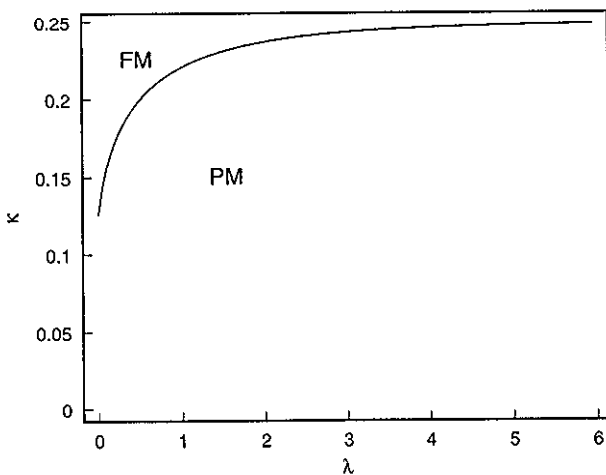


FIG. 1.  $\kappa_c$  for the FM-PM transition at  $y = 0$ .

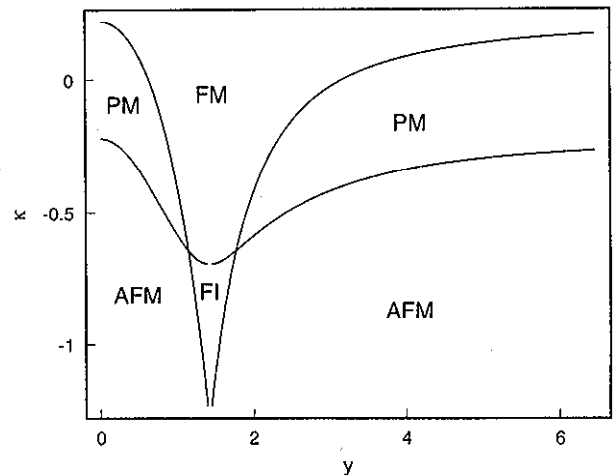


FIG. 2. The phase diagram for  $\lambda = 1$ . All phase transitions are second order.

Substituting Eqs. (21)–(23) into Eqs. (12) and (7) gives  $F_{\text{var}}$ .

There are four phases: (1) the ferromagnetic (FM) phase with  $\langle \phi_x^i \rangle \neq 0$ , (2) the paramagnetic (PM) phase with  $\langle \phi_x^i \rangle = 0$ , (3) the antiferromagnetic (AFM) phase with  $\langle \xi_x \phi_x^i \rangle \neq 0$  (where  $\xi_x = (-1)^{x_1+x_2+\dots+x_d}$ ), and (4) the ferrimagnetic (FI) phase in which  $\langle \phi_x^i \rangle \neq 0$  and  $\langle \xi_x \phi_x^i \rangle \neq 0$ . In the MFA these phases are indicated by the value of  $H^k$  which minimizes the variational free energy. In the FM phase  $H^k \neq 0$ , while for the PM phase  $H^k = 0$ . To see the AFM phase the action must be transformed so as to make the staggered magnetization  $\langle \xi_x \phi_x^i \rangle$  accessible. Since the action is invariant under  $\phi_x \rightarrow \xi_x \phi_x$ ,  $\psi_x \rightarrow \exp(i\pi 2\xi_x/2)\psi_x$ ,  $y \rightarrow iy$ ,  $\kappa \rightarrow -\kappa$ , the action obtained by this transformation will have AFM order if  $H^k \neq 0$ . Therefore, the MFA variational action for the AFM is given by Eq. (12) with  $y \rightarrow iy$ ,  $\kappa \rightarrow -\kappa$ . The FI phase is indicated by the existence of FM and AFM order at the same point.

The strong coupling regime is reached by expanding the fermionic determinant in  $1/y$  rather than  $y$ . In this expansion  $K_{xy}$  appears rather than  $K_{xy}^{-1}$ , and so the  $1/d$  approximation of the propagator is not needed. Aside from this difference, the free energy is computed in the same manner as the weak coupling version. Therefore the strong coupling variational free energy is obtained making the replacement  $y \rightarrow d/2y$  in Eq. (12).

The second order phase transitions are found by setting  $\frac{\delta^2}{\delta H^2} F_{\text{var}}|_{H=0} = 0$ , which is why it was sufficient to compute  $F_{\text{var}}$  to  $O(H^2)$ . For weak coupling this gives

$$\text{FM-PM: } \kappa_c = \frac{P_3}{P_5 d} - \frac{2^{d/2} N_F}{d^2} y^2 + \frac{2^{d/2} N_F P_5}{P_3 d^3} \left( \frac{1}{2d} - 1 \right) y^4; \quad (24)$$

$$\text{AFM-PM: } \kappa_c = -\frac{P_3}{P_5 d} - \frac{2^{d/2} N_F}{d^2} y^2 - \frac{2^{d/2} N_F P_5}{P_3 d^3} \left( \frac{1}{2d} - 1 \right) y^4. \quad (25)$$

The figures illustrate the above results. Figure 1 shows

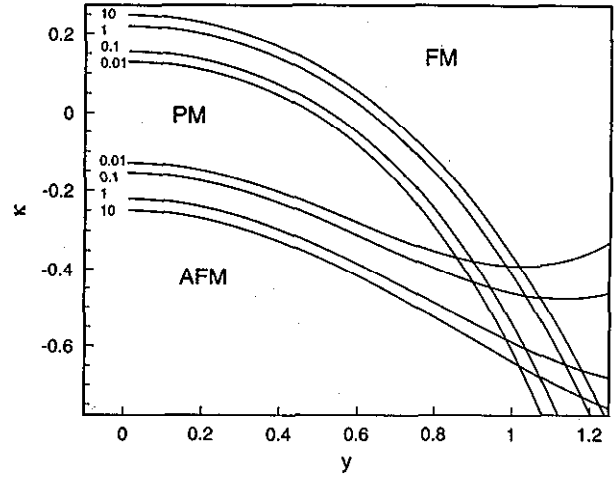


FIG. 3. Second order  $\kappa_c$ 's for various values of  $\lambda$  as indicated by the labels. The  $\lambda = 0.01, 10$  lines are very nearly the same as those for  $\lambda = 0, \infty$ , respectively.

$\kappa_c$  as a function of  $\lambda$  at  $y = 0$  for the FM-PM transition. (At  $y = 0$ ,  $\kappa_c$  for the AFM-PM transition is simply the negative of  $\kappa_c$  for the FM-PM transition.) In agreement with previous results [6,10],  $\kappa_c \rightarrow 1/8$  as  $\lambda \rightarrow 0$ , and  $\kappa_c \rightarrow 1/4$  as  $\lambda \rightarrow \infty$ . Figure 2 shows the complete phase diagram for  $\lambda = 1$ , which appears qualitatively similar to the  $\lambda = \infty$  case. The one difference from the  $\lambda = \infty$  case is that the PM region has shrunk. Figure 3 shows the  $\kappa_c$ 's as a function of  $y$  for several values of  $\lambda$  between 0.01 and 10. As  $\lambda$  is decreased, the phase diagram remains qualitatively the same as the  $\lambda = \infty$  case, although the PM region shrinks in both the  $y$  and  $\kappa$  directions. All phase transitions remain second order, and there is no evidence of new phases. Also,  $\kappa_c$  saturates for  $\lambda = 0.01, 10$ , with little change in  $\kappa_c$  as  $\lambda \rightarrow 0, \infty$ .

In addition to the MFA errors of order  $1/d^2$ , the errors in the expansion of the fermionic determinant are of order  $y^6$ . For  $y \approx 1$  the results should break down, although a comparison of the  $\lambda = \infty$  results with those from Monte Carlo simulation show good agreement through the intermediate coupling region.

[1] CDF Collaboration, F. Abe *et al.*, Phys. Rev. D **50**, 2966 (1994); Phys. Rev. Lett. **73**, 225 (1994).  
 [2] M. A. Stephanov and M. M. Tsy-pin, Phys. Lett. B **261**, 109 (1991); **242**, 432 (1990); **236**, 344 (1990).  
 [3] M. A. Stephanov and M. M. Tsy-pin, Zh. Eksp. Teor. Fiz. **97**, 409 (1990).  
 [4] T. Ebihara and K. Kondo, Prog. Theor. Phys. **87**, 1019 (1992).  
 [5] W. Bock *et al.*, Nucl. Phys. **344**, 207 (1990); W. Bock and A. K. De, Phys. Lett. B **245**, 207 (1990).  
 [6] H. Kuhnelt, C. B. Lang, and G. Vones, Nucl. Phys. **B230**, 16 (1984); I. Montvay, Phys. Lett. **150B**, 441 (1985); J. Jersak *et al.*, Phys. Rev. D **32**, 2761 (1985).  
 [7] R. E. Shrock, Phys. Lett. B **180**, 268 (1986); P. H.

Damgaard and U. M. Heller, Phys. Lett. **164B**, 121 (1985); Y. Sugiyama and T. Yokota, *ibid.* **168B**, 386 (1986); Prog. Theor. Phys. **76**, 667 (1986); T. Munehisa and Y. Munehisa, Nucl. Phys. **B215**, 508 (1983); Y. Sugiyama and K. Kanaya, Prog. Theor. Phys. **73**, 176 (1985).  
 [8] A. Hasenfratz, K. Jansen, and Y. Shen, Nucl. Phys. **B394**, 527 (1993).  
 [9] J. M. Drouffe and J. B. Zuber, Phys. Rep. **102**, 1 (1983), and references therein.  
 [10] A. Hasenfratz *et al.*, Nucl. Phys. **B365**, 79 (1991); P. R. Gerber and M. E. Fisher, Phys. Rev. B **10**, 4697 (1974); K. Jansen *et al.*, Nucl. Phys. **B265**, 129 (1986).